

1 **Contrasting responses of phytoplankton productivity between coastal and offshore**
2 **surface waters in the Taiwan Strait and the South China Sea to ~~future~~**
3 **~~CO₂-induced~~short-term seawater acidification**

4
5 Guang Gao¹, Tifeng Wang¹, Jiazhen Sun¹, Xin Zhao¹, Lifang Wang¹, Xianghui Guo¹,
6 Kunshan Gao^{1,2*}

7 ¹State Key Laboratory of Marine Environmental Science & College of Ocean and Earth
8 Sciences, Xiamen University, Xiamen 361005, China

9 ²Co-Innovation Center of Jiangsu Marine Bio-industry Technology, Jiangsu Ocean
10 University, Lianyungang 222005, China

11

12 *Corresponding author: ksgao@xmu.edu.cn

13

14 **Abstract**

15 ~~Future CO₂-induced ocean acidification (OA)~~Seawater acidification (SA) has been
16 documented to either inhibit or enhance or result in no effect on marine primary
17 productivity (PP). In order to examine effects of ~~OA-SA in changing environments under~~
18 ~~multiple drivers~~, we investigated the influences of SAOA (a decrease of 0.4 pH_{total} units
19 with corresponding CO₂ concentrations ranged 22.0–39.7 μM) on PP through
20 deck-incubation experiments at 101 stations in the Taiwan Strait and the South China Sea
21 (SCS), including ~~the coastal zone~~, the continental shelf and slope, as well as deep-water
22 basin. The daily ~~net~~ primary productivities in surface seawater under incident solar
23 radiation ranged from 17–306 μg C (μg Chl *a*)⁻¹ d⁻¹, with the responses of PP to OA-SA
24 being region-dependent and the OA-SA-induced changes varying from -88.03%
25 (inhibition) to 56.877% (enhancement). The OA-SA-treatment stimulated PP in surface
26 waters of coastal, estuarine and shelf waters, but suppressed it in the South China Sea
27 basin. Such OA-SA-induced changes in PP were significantly related to ~~NO_x (the sum of~~
28 ~~NO₃⁻ and NO₂⁻) availability~~, in situ pH and solar radiation in surface seawater, but
29 negatively related to salinity changes. Our results indicate that phytoplankton cells are
30 more vulnerable to pH drop in oligotrophic waters. Contrasting responses of
31 phytoplankton productivity in different areas suggest that SA impacts on marine primary
32 productivity are region-dependent and regulated by local environments.~~Considering high-~~
33 ~~nutrient and low salinity in coastal waters and reduced nutrient availability in pelagic-~~

~~zones with the progressive stratification associated with ocean warming, our results imply that future OA will enhance PP in coastal waters but decrease it in pelagic oligotrophic zones.~~

Keywords: CO₂; Taiwan Strait; ~~ocean~~ seawater acidification; photosynthesis; primary productivity; South China Sea

1 Introduction

The oceans have absorbed about one-third of anthropogenically released CO₂, which increased dissolved CO₂ and decreased pH of seawater (Gattuso et al., 2015), leading to ocean acidification (OA). This process is ongoing and likely intensifying (IPCC, 2019). OA has been shown to result in profound influences on marine ecosystems (see the reviews and literature therein, Mostofa et al., 2016; Doney et al., 2020). Marine photosynthetic organisms, which contribute about half of the global primary production, are also being affected by OA (see the reviews and literatures therein, Riebesell et al., 2018; Gao et al., 2019a). In addition to the slow change of ocean acidification, some processes, such as freshwater inputs, upwelling, typhoon and eddies, can lead to instantaneous CO₂ rising and seawater acidification (Moreau et al., 2017; Yu et al., 2020). ~~It is of general concern that the oceans are going to take more or less CO₂ with progressive OA, since the amount of CO₂ uptake by the oceans is essential to predict global and ocean warming trends. Therefore,~~ Since seawater acidification occurs in many locations of ocean, it is important to understand the responses of the key players of

54 marine biological CO₂ pump, the phytoplankton, to ~~OA seawater acidification and other~~
55 ~~climate change drivers~~.

56 Elevated CO₂ is well recognized to lessen the dependence of algae and
57 cyanobacteria on energy-consuming CO₂ concentrating mechanisms (CCMs) which
58 concentrate CO₂ around Rubisco, the key site for photosynthetic carbon fixation (Raven
59 & Beardall, 2014 and references therein; Hennon et al., 2015). The energy freed up from
60 the down-regulated CCMs under increased CO₂ concentrations can be applied to other
61 metabolic processes, resulting in a modest increase in algal growth (Wu et al., 2010;
62 Hopkinson et al., 2011; Xu et al., 2017). Accordingly, elevated CO₂ availability could
63 potentially enhance marine primary productivity (Schippers et al., 2004). For instance,
64 across 18 stations in the central Atlantic Ocean primary productivity was stimulated by
65 15–19% under elevated dissolved CO₂ concentrations up to 36 μM (Hein and
66 Sand-Jensen 1997). On the other hand, neutral effects of ~~OA seawater acidification (SA)~~
67 on growth rates of phytoplankton communities were reported in five of six CO₂
68 manipulation experiments in the coastal Pacific (Tortell et al., 2000). Furthermore,
69 simulated future ~~OA-SA~~ reduced surface PP in pelagic surface waters of Northern SCS
70 and East China Sea (Gao et al., 2012). It seems that the impacts of ~~OA-SA~~ on PP could be
71 region-dependent. The varying effects of ~~OA-SA~~ may be related to the regulation of other
72 factors such as light intensity (Gao et al., 2012), temperature (Holding et al., 2015),
73 nutrients (Tremblay et al., 2006) and community structure (Dutkiewicz et al., 2015).

74 Taiwan Strait of the East China Sea, located between southeast Mainland China and
75 the Taiwan Island, is an important channel in transporting water and biogenic elements
76 between the East China Sea (ECS) and the South China Sea (SCS). Among the Chinese
77 coastal areas, the Taiwan Strait is distinguished by its unique location. In addition to
78 riverine inputs, it also receives nutrients from upwelling (Hong et al., 2011). Primary
79 productivity is much higher in coastal waters than that in pelagic-basin zones due to
80 increased supply of nutrients through river runoff and upwelling (Chen, 2003; Cloern et
81 al., 2014). The South China Sea (SCS), located from the equator to 23.8°N, from 99.1 to
82 121.1°E and encompassing an area of about 3.5×10^6 km², is one of the largest marginal
83 seas in the world. As a marginal sea of the Western Pacific Ocean, it has a deep
84 semi-closed basin (with depths > 5000 m) and wide continental shelves, characterized by
85 a tropical and subtropical climate (Jin et al., 2016). Approximately 80% of ocean organic
86 carbon is buried in the Earth's continental shelves and therefore continental margins play
87 an essential role in the ocean carbon cycle (Hedges & Keil, 1995). Investigating how
88 ocean acidification affects primary productivity in the Taiwan Strait and the SCS could
89 help us to understand the contribution of marginal seas to carbon sink under the future
90 CO₂-increased scenarios. Although small-scale studies on OA-SA impacts have been
91 conducted in the ESC and the SCS (Gao et al., 2012, 2017), our understanding of how
92 OA-SA affects PP in marginal seas is still fragmentary and superficial. In this study, we
93 conducted three cruises in the Taiwan Strait and the SCS, covering an area of 8.3×10^5

94 km², and aimed to provide in-depth insight into how ~~OA-SA~~ and/or episodic pCO₂ rise
95 affects PP in marginal seas with comparisons to other types of waters.

96 **2 Materials and Methods**

97 **2.1 Investigation areas**

98 To study the impacts of projected ~~OA-SA~~ (dropping by ~0.4 pH) by the end of this
99 century (RCP8.5) on marine primary productivity in different areas (Gattuso et al., 2015),

100 we carried out deck-based experiments during the 3 cruises supported by National
101 Natural Science Foundation of China (NSFC), which took place in the Taiwan Strait (Jul
102 14th–25th, 2016), the South China Sea basin (Sep 6–24th, 2016), and the West South China
103 Sea (Sep 14th to Oct 24th, 2017), respectively. The experiments were conducted at 101
104 stations with coverage of 12 °N–26 °N and 110 °E–120 °E (Fig. 1). Investigation areas

105 include ~~the coastal zone (< 50 m)~~, the continental shelf (~~500~~–200 m, 22 stations) and the
106 slope (200–~~1000~~–3400 m, 44 stations), and the vast deep-water basin (> ~~1000~~–3400 m, 35
107 stations). In the continental shelf, the areas with depth < 50 m are defined as coastal
108 zones (9 stations).

109 **2.2 Measurements of temperature and carbonate chemistry parameters**

110 The temperature and salinity of surface seawater at each station were monitored with
111 an onboard CTD (Seabird, USA). pH_{NBS} was measured with an Orion 2-Star pH meter
112 (Thermo scientific, USA) that was calibrated with standard National Bureau of Standards
113 (NBS) buffers (pH=4.01, 7.00, and 10.01 at 25.0 °C; Thermo Fisher Scientific Inc., USA).

114 After the calibration, the electrode of pH meter was kept in surface seawater for half an
115 hour and then the formal measurements were conducted. The analytical precision was
116 ± 0.001 . Total alkalinity (TA~~K~~) was determined using Gran titration on a 25-mL sample
117 with a TA analyzer (AS-ALK1, Apollo SciTech, USA) that was regularly calibrated with
118 certified reference materials supplied by A. G. Dickson at the Scripps Institution of
119 Oceanography (Gao et al., 2018a). The analytical precision was $\pm 2 \mu\text{mol kg}^{-1}$. CO_2
120 concentration in seawater and the pH_{Total} (pH_{T}) values was calculated by using CO2SYS
121 (Pierrot et al., 2006) with the input of pH_{NBS} and TA~~K~~ data.

122 **~~2.3 Nutrient measurement~~**

123 ~~Surface seawater was collected from the Conductivity Temperature Depth (CTD)-~~
124 ~~rosette/Niskin bottles with a clean 125 mL HDPE (High Density Polyethylene) sample~~
125 ~~container. The nitrate and nitrite concentrations in seawater were then measured with a~~
126 ~~Technicon AA3 Auto Analyzer (Bran Lube, GmbH, Germany). The quantitative limits~~
127 ~~for nitrate and nitrite were $0.1 \mu\text{mol L}^{-1}$ and $0.04 \mu\text{mol L}^{-1}$, respectively. We used~~
128 ~~certified reference materials (CRMS) (<https://www.jamstec.go.jp/scor/>) as external~~
129 ~~quality checks, and the analytical precision was better than $\pm 1\%$ during the whole cruise.~~
130 ~~Nutrient measurement was conducted in the cruise of the South China Sea basin. Due to~~
131 ~~the limit of human resources, it was not conducted in the other two cruises.~~

132 **~~2.4.3 Solar radiation~~**

133 The incident solar radiation intensity during the cruises was recorded with an

134 Eldonet broadband filter radiometer (Eldonet XP, Real Time Computer, Germany). This
135 device has three channels for PAR (400–700 nm), UV-A (315–400 nm) and UV-B (280–
136 315 nm) irradiance, respectively, which records the means of solar radiations over each
137 minute. The instrument was fixed at the top layer of the ship to avoid shading.

138 **2.5.4 Determination of primary productivity**

139 Surface seawater (0–1m) was collected a 10 L acid-cleaned (1 M HCl) plastic bucket
140 and pre-filtered (200 µm mesh size) to remove large grazers. To prepare high CO₂ (HC)
141 seawater, CO₂-saturated seawater was added into pre-filtered seawater until a decrease of
142 ~0.4 units in pH (corresponding CO₂ concentrations being 22.0–39.7 µM) was
143 approached (Gattuso et al., 2010). Seawater that was collected from the same location as
144 PP and filtered by cellulose acetate membrane (0.22 µm) was used to make the
145 CO₂-saturated seawater, which was made by directly flushing with pure CO₂ until pH
146 reached around 4.50. When saturated-CO₂ seawater was added to the HC treatment,
147 equivalent filtered seawater (without flushing with CO₂) was also added to the AC
148 treatment as a control. The ratios of added saturated-CO₂ seawater to incubation seawater
149 were about 1:1000. Seawater was incubated within half an hour after they were
150 collected~~The same amount of filtered seawater (0.22 µm) was added into the pre-filtered~~
151 ~~seawater setting as ambient CO₂-(AC) control.~~ Prepared AC and HC seawater was
152 allocated into 50-mL quartz tubes in triplicate, inoculated with 5 µCi (0.185 MBq)
153 NaH¹⁴CO₃ (ICN Radiochemicals, USA), and then incubated for 24 h (over a day-night

带格式的：上标

154 cycle) under 100 % incident solar irradiances in a water bath for temperature control by
155 running through surface seawater. Due to heating by the deck, the temperatures in the
156 water bath were 0–2 °C higher than in situ surface seawater temperatures. TA and pH of
157 seawater before and after 24h incubation were measured to monitor the changes of
158 carbonate systems. After the incubation, the cells were filtered onto GF/F filters
159 (Whatman) and immediately frozen at –20 °C for later analysis. In the laboratory, the
160 frozen filters were transferred to 20 mL scintillation vials, thawed and exposed to HCl
161 fumes for 12 h, and dried (55 °C, 6 h) to expel non-fixed ¹⁴C, as previously reported (Gao
162 et al., 2017). Then 3 mL scintillation cocktail (Perkin Elmer®, OptiPhase HiSafe) was
163 added to each vial. After 2 h of reaction, the incorporated radioactivity was counted by a
164 liquid scintillation counting (LS 6500, Beckman Coulter, USA). The carbon fixation for
165 24 h incubation was taken as chlorophyll (Chl) *a*-normalized daily ~~net~~-primary
166 productivity (PP, μg C (μg Chl *a*)⁻¹) (Gao et al., 2017). The changes (%) of PP induced by
167 ocean acidification were expressed as (PP_{HC}–PP_{AC})/PP_{AC}×100, where PP_{HC} and PP_{AC} are
168 the ~~net~~-daily primary productivity under HC and AC, respectively.

169 **2.6.5 Chl *a* measurement**

170 Pre-filtered (200 μm mesh size) surface seawater (500–2000 mL) at each station was
171 filtered onto GF/F filter (25 mm, Whatman) and then stored at -80 °C. After returning to
172 laboratory, phytoplankton cells on the GF/F filter were extracted overnight in absolute
173 methanol at 4 °C in darkness. After centrifugation (5000 *g* for 10 min), the absorption

174 values of the supernatants were analyzed by a UV–VIS spectrophotometer (DU800,
175 Beckman, Fullerton, California, USA). The concentration of chlorophylls *a* (Chl *a*) was
176 calculated according to Porra (2002).

177 **2.7.6 Data analysis**

178 The data of environmental parameters were expressed in raw and the data of PP were
179 the means of triplicate incubations. Two-way analysis of variance (ANOVA) was used to
180 analyze the effects of ~~OA~~SA and location on PP. Least significant difference (LSD) was
181 used to for *post hoc* analysis. Linear fitting analysis was conducted with Pearson
182 correlation analysis to assess the relationship between PP and environmental factors. A 95%
183 confidence level was used in all analyses.

184 **3 Results**

185 During the cruises, surface temperature ranged from 25.0 to 29.9 °C in the Taiwan
186 Strait and from 27.1 to 30.2 °C in the South China Sea (Fig. 2a). Surface salinity ranged
187 from 30.0 to 34.0 in the Taiwan Strait and from 31.0 to 34.3 in the South China Sea (Fig.
188 2b). The lower salinities were found in the estuaries of Minjiang and Jiulong Rivers as
189 well as Mekong River-induced Rip current. High salinities were found in the SCS basin.
190 Surface pH_T changed between 7.99–8.20 in the Taiwan Strait with the higher values in
191 the estuary of Minjiang River (Fig. 2c). Compared to the Taiwan Strait, the South China
192 Sea had lower surface pH (7.91–8.08) with the lowest value near the island in the
193 Philippines. TA~~TK~~ ranged from 2100 to 2359 μmol ~~L~~kg⁻¹ SW in the Taiwan Strait and

194 2126 to 2369 $\mu\text{mol kg}^{-1} \text{ SW}$ in the South China Sea (Fig. 2d). The lowest value occurred
195 in the estuary of Minjiang River. CO_2 concentration in surface seawater changed from
196 6.4–13.3 $\mu\text{M kg}^{-1} \text{ SW}$ in the Taiwan Strait, and 9.3–14.3 $\mu\text{M kg}^{-1} \text{ SW}$ in the SCS (Fig. 1e).
197 It showed an opposite pattern to surface pH, with the lowest value in the estuary of
198 Minjiang River in the Taiwan Strait and highest value in near the islands in the
199 Philippines in the South China Sea. During the PP investigation period, the daytime mean
200 PAR intensity ranged from 126.6 to 145.2 $\text{W m}^{-2} \text{ s}^{-1}$ in the Taiwan Strait and 37.3 to 150.0
201 $\text{W m}^{-2} \text{ s}^{-1}$ in the SCS (Fig. 2f).

202 The concentration of Chl *a* ranged from 0.11 to 12.13 $\mu\text{g L}^{-1}$ in the Taiwan Strait (Fig.
203 3). The highest concentration occurred in the estuary of the Minjiang River. The
204 concentration of Chl *a* in the SCS ranged from 0.037 to 7.43 $\mu\text{g L}^{-1}$. The highest
205 concentration was found in the coastal areas of Guangdong province in China. For both
206 the Taiwan Strait and the SCS, there were high Chl *a* concentrations ($> 1.0 \mu\text{g L}^{-1}$) in
207 coastal areas, particularly in the estuaries of the Minjing River, Jiulong River and Pearl
208 River. On the contrary, Chl *a* concentrations in offshore areas were lower than $0.2 \mu\text{g L}^{-1}$.

209 Surface primary productivity changed from 99–302 $\mu\text{g C } (\mu\text{g Chl } a)^{-1} \text{ d}^{-1}$ in the
210 Taiwan Strait, and from 17–306 $\mu\text{g C } (\mu\text{g Chl } a)^{-1} \text{ d}^{-1}$ in the South China Sea (Fig. 4).
211 High surface primary productivity ($> 200 \mu\text{g C } (\mu\text{g Chl } a)^{-1} \text{ d}^{-1}$) was found in the
212 estuaries of the Minjing River, Jiulong River, and Pearl River and areas near the East of
213 Vietnam. In pelagic-basin zones, the surface primary productivity was usually lower than

214 100 $\mu\text{g C}$ ($\mu\text{g Chl } a$)⁻¹ d⁻¹.

215 ~~Through a~~ series of onboard CO₂-enrich experiments in the investigated regions

216 were conducted during three cruises. In the high CO₂ treatments, pH_{total} had a decrease of

217 0.34–0.43 units, while pCO₂ and CO₂ had an increase of 676–982 μatm and 17–25 μM ,

218 kg⁻¹ SW, respectively (Table S1). Carbonate chemistry parameters after 24 h of

219 incubation were stable ($\Delta\text{pH} < 0.06$, $\Delta\text{TA} < 53 \mu\text{mol kg}^{-1}$ SW), indicating the

220 successful manipulation (Table S1). ~~we~~ It was observed that instantaneous effects of ~~the~~

221 elevated pCO₂ on primary productivity of surface phytoplankton community in all

222 investigated regions ranged from -88.03% (inhibition) to 56.877% (promotion), revealing

223 significant regional differences (ANOVA, $F_{(100, 404)} = 4.103$, $p < 0.001$, Fig. 5). Among

224 101 stations, 70 stations showed insignificant ~~OA-SA~~ effects. ~~OA-SA~~ increased PP at 6

225 stations and reduced PP at 25 stations. Positive effects of ~~OA-SA~~ on surface primary

226 productivity ~~was-were~~ observed in the Taiwan Strait and the western SCS (Fig. 5,

227 red-yellow shading areas), with the maximal enhancement of 56.97% in the station

228 approaching ~~the~~ Mekong River plume (LSD, $p < 0.001$). Reductions in PP induced by the

229 elevated CO₂ ~~was-were~~ mainly found in the central SCS basin within the latitudes of 10

230 °N to 14 °N and the longitudes of 114.5 °E to 118 °E (Fig. 5, blue-purple shading areas),

231 with inhibition rates ranging from 24.02% to 88.03% (Fig. 5, LSD, $p < 0.05$). These

232 results showed a region-related effect of ~~OA-SA~~ on photosynthetic carbon fixation of

233 surface phytoplankton assemblages. Overall, the elevated pCO₂ had neutral or positive

带格式的: 下标

带格式的: 下标

带格式的: 下标

带格式的: 下标

234 effects on primary productivity in the continental shelf and slope regions ~~nearshore~~
235 ~~waters~~, while having adverse effects in the deep-water basin ~~pelagic waters~~.

236 By analyzing the correlations between OA-SA-induced PP changes and regional
237 environmental parameters, we found that OA-SA-induced changes in phytoplankton
238 primary productivity was significantly positively related with *in situ* pH ($p < 0.001$, $r =$
239 0.379), ~~NO_x availability (the concentrations of NO₃⁻ + NO₂⁻ at the bottom of upper~~
240 ~~mixing layers as they were unmeasurable in the surface water, $p = 0.002$, $r = 0.727$) and,~~
241 PAR density ($p = 0.002$, $r = 0.311$) ~~and primary productivity ($p = 0.004$, $r = 0.284$)~~ (Fig. 6
242 and Table S1). On the other hand, the influence induced by OA-SA was negatively related
243 to salinity that ranged from 30.00 to 34.28 ($p < 0.001$, $r = -0.418$).

244 **4 Discussion**

245 In the present study, we found that the elevated pCO₂ and associated pH drop
246 increased or did not affect PP in ~~coastal~~ the continental shelf and slope waters but
247 reduced it in pelagic-basin waters. Our results suggested that the enhanced effects of the
248 OA-SA treatment on photosynthetic carbon fixation depend on regions of different
249 physicochemical conditions, ~~including pH, light intensity and salinity. Higher levels of~~
250 ~~nutrients due to runoffs or upwellings should be mainly responsible for the enhancement.~~
251 ~~On the other hand, such stimulation could be related to higher UV attenuation in these~~
252 ~~coastal waters that contain more organic matters (Hader et al., 2015), since we employed~~
253 ~~UV transparent vessels for the incubations.~~ In addition, coastal diatoms appear to benefit

254 | more from ~~OA-SA~~ than pelagic ones (Li et al., 2016). Therefore, community structure
255 | differences might also be responsible for the differences of the short-term high
256 | CO₂-induced acidification between coastal and ~~pelagic-basin~~ waters.

257 | ~~OA-SA~~ is deemed to have two kinds of effects at least (Xu et al., 2017; Shi et al.,
258 | 2019). The first one is the enrichment of CO₂, which is usually beneficial for
259 | photosynthetic carbon fixation and growth of algae because insufficient ambient CO₂
260 | limits algal photosynthesis (Hein & Sand-Jensen, 1997; Bach & Taucher, 2019). The
261 | other effect is the decreased pH which could be harmful because it disturbs the acid-base
262 | balance between extracellular and intracellular environments. For instance, the decreased
263 | pH projected for future ~~OA-SA~~ was shown to reduce the growth of the diazotroph
264 | *Trichodesmium* (Hong et al., 2017), decrease PSII activity by reducing ~~the~~ removal rate
265 | of PsbD (D2) (Gao et al., 2018b) and increase mitochondrial and photo-respirations in
266 | diatoms and phytoplankton assemblages (Yang and Gao 2012, Jin et al., 2015). In
267 | addition, ~~OA-SA~~ could reduce the ~~RuBisCO-Rubisco~~ transcription of diatoms, which also
268 | contributed to the decreased growth (Endo et al., 2015). Therefore, the net impact of ~~OA-~~
269 | ~~SA~~ depends on the balance between its positive and negative effects, leading to enhanced,
270 | inhibited or neutral influences, as reported in diatoms (Gao et al., 2012, Li et al., 2021)
271 | and phytoplankton assemblages in the Arctic and subarctic shelf seas (Hoppe et al., 2018),
272 | the North Sea (Eberlein et al., 2017) and the South China Sea (Wu and Gao 2010, Gao et
273 | al., 2012). The balance of positive and negative effects of SA can be regulated by other

274 factors, including pH, light intensity, salinity, population structure, etc. (Gao et al., 2019a,
275 b; Xie et al., 2022).

276 In the present study, ~~OA-SA~~ increased or did not affect PP in coastal waters but
277 reduced it in offshore waters, ~~which is. This is~~ significantly related to ~~nutrient~~
278 ~~availability~~ pH, light intensity and salinity (Fig. 6d). The effect of SA changed from
279 negative to positive with the increase of local pH. The higher pH occurred in coastal
280 zones; which may be caused by higher biomass of phytoplankton (Fig. 3). Higher pH
281 caused by intensive photosynthesis of phytoplankton is companied with decreased CO₂
282 levels. In this case, CO₂ is more limited for photosynthesis of phytoplankton compared to
283 lower pH. Therefore, SA could stimulate primary productivity via supplying more
284 available CO₂ (Hurd et al., 2019). On the other hand, lower pH occurred in deep-water
285 basin. Lower pH represents higher CO₂ availability. CO₂ is not limited or less limited in
286 this case. Therefore, more CO₂ brought by SA may not benefit photosynthesis of
287 phytoplankton. Instead, decreased pH accompanied by SA may inhibit photosynthesis or
288 growth of phytoplankton, which is found in cyanobacteria (Hong et al., 2017).
289 Furthermore, the negative effects of SA are particularly significant when nutrient is
290 limited (Li et al., 2018). The nutrient levels in basin are usually lower than shelf (Yuan et
291 al., 2011; Lu et al., 2020; Du et al., 2021), which may exacerbate the negative effects of
292 OA in the basin zone.

293 The negative effects of SA disappeared with the increase of light intensity in this

带格式的: 下标

294 study. This results in inconsistent with Gao et al (2012)' study, in which SA increased
295 photosynthetic carbon fixation of three diatoms (*Phaeodactylum tricornutum*,
296 *Thalassiosira pseudonana* and *Skeletonema costatum*) under lower light intensities but
297 increased it under higher light intensities. The divergent findings may be due to different
298 population structure that varies in different areas. Coastal zones where nutrients are
299 relatively sufficient usually have abundant diatoms while picophytoplanktons mainly
300 *Prochlorococcus* and *Synechococcus*, dominate oligotrophic areas (Xiao et al., 2018,
301 Zhong et al., 2020). In this study, most investigated areas are oligotrophic and thus the
302 response of local phytoplankton to the combination of light intensity and SA may be
303 different from diatoms. It is worth noting that the samples were not mixed down in the
304 water bath in the present study and the 100% incident solar irradiances may have high
305 light stress on cells. Lower incident solar irradiances or some devices can be used to
306 simulate seawater mixing in future studies. Negative correlation between Θ SA-induced
307 changes of PP and salinity was found in this study. ~~While little has been documented on~~
308 ~~the relationship between salinity and OA (Wulff et al., 2018; Sugie et al., 2020; Xu et al.,~~
309 ~~2020) , lowered~~The decrease of salinity (from 35 to 30) ~~salinity~~ has been shown to
310 ~~alleviate the impact~~negative effect of Θ SA on photosynthetic carbon fixation of a
311 ~~coccolithorphorid~~ *Emiliana huxleyi* (Xu et al., 2020) although the potential mechanisms
312 remain unknown. On the other hand, the change of salinity (from 6 to 3) did not affect
313 effective quantum yield of microplanktonic community in the Baltic Sea grown under

带格式的：字体：倾斜

带格式的：字体：倾斜

带格式的: 下标

314 different CO₂ levels (Wulff et al., 2018). In this study, ~~Nevertheless, we presume that the~~
315 ~~enhanced~~ negative relationship between salinity and SA effects ~~PP could~~ may be mainly
316 be related to nutrient availability local pH because lower salinity occurred in coastal
317 waters usually companies with high nutrient levels where seawater pH was higher while
318 the basin zone had higher salinities and lower pH (Li et al., 2011).

319 ~~with that the inhibitory effect was minimized when NO_x availability increased.~~
320 Riverine inputs, including the Minjiang River, Jiulong River, Pearl River, and Mekong
321 River, are the primary source of nutrients in the coastal and shelf zones, resulting in
322 higher concentrations of nutrients and lower salinity in these waters (Xiao et al., 2018). It
323 was reported that elevated pCO₂ decreased net organic carbon production of
324 natural plankton community in nutrient-depleted waters (Yoshimura et al., 2010).
325 Furthermore, OA did not affect the specific growth rate of a diatom under N-replete
326 condition but reduced it under N-limited condition (Li et al., 2018). The alleviating effect
327 of nutrient enrichment on OA-induced stress could be multifaceted. Firstly, algae could
328 cope with the acid-base perturbation caused by OA through active proton pumps
329 (McNicholl et al., 2019). The operation of such proton pumps need some essential
330 proteins, such as plasma membrane H⁺-ATPase, whose synthesis is nutrient-dependent
331 (Taylor et al., 2012; Xu et al., 2017). Secondly, it has been shown that nutrient
332 enrichment could accelerate the repair rate of PSII via synthesizing the key proteins such
333 as PsbA (D1), and PsbD (D2) (Geider et al., 1993; Li et al., 2015). Thirdly, nitrogen

334 ~~enrichment could significantly increase the synthesis and content of photosynthetic~~
335 ~~pigments including Chl *a*, phycoeyanin, and phycoerythrin (Johnson & Carpenter, 2018;~~
336 ~~Gao et al., 2019b), contributing to high photosynthetic activity under stressful~~
337 ~~environmental conditions. Negative correlation between OA-induced changes of PP and~~
338 ~~salinity was found in this study. While little has been documented on the relationship~~
339 ~~between salinity and OA (Wulff et al., 2018; Sugie et al., 2020; Xu et al., 2020), lowered~~
340 ~~salinity has been shown to alleviate the impact of OA on a coccolithoroid (Xu et al.,~~
341 ~~2020). Nevertheless, we presume the enhanced PP could mainly be related to nutrient~~
342 ~~availability because lower salinity in coastal waters usually accompanies with high nutrient~~
343 ~~levels (Li et al., 2011). In addition, local pH may be another factor that affects the~~
344 ~~impacts of OA. There are diurnal and seasonal fluctuations of pH in coastal waters and~~
345 ~~phytoplankton that adapt well to the fluctuant pH environments would be tolerant to the~~
346 ~~decreased pH caused by OA (Flynn et al., 2012, Li et al., 2016). On the other hand, the~~
347 ~~surface pH in the ocean basin is relatively stable, with a varied range of only -0.024 over~~
348 ~~a month (Hofmann et al., 2011). Therefore, the phytoplankton cells living in these~~
349 ~~environments could be more sensitive to pH drop due to elevated pCO₂ (Li et al., 2016).~~

350

351 The specific environmental conditions have profound effects on shaping diverse
352 dominant phytoplankton groups (Boyd et al., 2010). Larger eukaryotic groups (especially
353 diatoms) usually dominate the complex coastal regions, while picophytoplanktons

354 (*Prochlorococcus* and *Synechococcus*), characterizing with more efficient nutrients
355 uptake, dominate the relatively stable offshore waters (Dutkiewicz et al., 2015). In
356 summer and early autumn, previous investigations demonstrated that diatoms dominated
357 in the northern waters and the Taiwan Strait (coastal and shelf regions) with the high
358 abundance of phytoplankton, which are consistent with our Chl *a* data; *Prochlorococcus*
359 and *Synechococcus* dominated in the SCS basin and the north of SCS (slope and basin
360 regions) (Xiao et al., 2018, Zhong et al., 2020). In addition, it has been reported that
361 larger cells benefit more from ~~OA-SA~~ because a thicker diffusion layer around the cells
362 limits the transport of CO₂ (Feng et al., 2010; Wu et al., 2014). In contrast, a thinner
363 diffusion layer and higher surface to volume ratio in smaller phytoplankton cells can
364 make them easier to transport CO₂ near the cell surface and within the cells, and therefore
365 picophytoplankton species are less CO₂-limited (Bao and Gao, 2021). Therefore, different
366 community structures between coastal and ~~pelagic-basin~~ areas could also be responsible
367 for the enhanced and inhibitory effects of ~~OA-SA~~. It is worth noting that seasonality may
368 also lead to the differential effects of SA on primary productivity since the Taiwan Strait
369 cruise was conducted in July and the cruises of the South China Sea basin and the West
370 South China Sea were conducted in September. The SST and solar PAR intensity of the
371 Taiwan Strait in July was 2–3 °C and 22 ± 22 W m⁻² s⁻¹ higher than that in September
372 (Zhang et al., 2008, 2009; Table S3). Although the effects of SA were not related to
373 temperature as shown in this study (Table S2), the higher solar radiation in July may

带格式的: 字体: 非倾斜

374 contribute to the positive effect of SA on primary productivity.

375 **5 Conclusions**

376 By investigating the impacts of the elevated pCO₂ on PP in the Taiwan Strait and the
377 SCS, we demonstrated that such short ~~OA~~SA-treatments induced changes in PP were
378 mainly related to ~~NO_x availability~~pH, light intensity and salinity based on Pearson
379 correlation coefficients, supporting the hypothesis that negative impacts of ~~OA~~SA on PP
380 increase from coastal to pelagic-basin waters (Gao et al., 2019a). In view of ocean climate
381 changes, strengthened stratification due to global warming would reduce the upward
382 transports of nutrients and ~~further reduce nutrient availability~~thus marine primary
383 productivity. The negative effect of SA in basin zones would further reduce primary
384 productivity, consequently, leading to exacerbating impacts of OA on PP in pelagic zones.
385 Meanwhile, PP in coastal ~~and/or upwelled~~ waters would be increased by SA. stimulated
386 ~~or non-affected by OA with continuous discharges of nutrients from terrestrial~~
387 ~~environments, which may imply higher PP and enhance frequency of harmful algal~~
388 ~~blooms in future oceans.~~

389 *Data availability.* All data are included in the article or Supplement.

390 *Author contributions.* KG and TW developed the original idea and designed research.

391 TW and JS carried out fieldwork. GG provided statistical analyses and prepared figures.

392 GG, KG, and XZ wrote the manuscript. All contributed to revising the paper.

393 *Competing interests.* The contact author has declared that neither they nor their

394 co-authors have any competing interests.

395 *Disclaimer.* Publisher's note: Copernicus Publications remains neutral with regard to

396 jurisdictional claims in published maps and institutional affiliations.

397 *Acknowledgements.* This work was supported by the National Natural Science Foundation
398 of China (41720104005, 41890803 and 42076154), and the Fundamental Research Funds
399 for the Central Universities (20720200111). The authors are grateful to the students He Li,
400 Xiaowen Jiang and Shanying Tong, and the laboratory technicians Xianglan Zeng and
401 Wenyan Zhao. We appreciate the NFSC Shiptime Sharing Project (project number:
402 41849901) for supporting the Taiwan Strait cruise (NORC2016-04). We appreciate the
403 chief scientists Yihua Cai, Huabin Mao and Chen Shi and the R/V Yanping II, Shiyan I
404 and Shiyan III for leading and conducting the cruises.

405 **References**

406 Bach, L. T., and Taucher, J.: CO₂ effects on diatoms: a synthesis of more than a decade of
407 ocean acidification experiments with natural communities, *Ocean Sci.*, 15,
408 1159-1175, 2019.

409 Bao, N., and Gao, K.: Interactive effects of elevated CO₂ concentration and light on the
410 picophytoplankton *Synechococcus*, *Front. Mar. Sci.*, 8, 1-7, 2021.

411 Boyd, P. W., Strzepek, R., Fu, F. X., and Hutchins, D. A.: Environmental control of open-
412 ocean phytoplankton groups: Now and in the future, *Limnol. Oceanogr.*, 55,
413 1353-1376, 2010.

414 Chen, C. T. A.: Rare northward flow in the Taiwan Strait in winter: A note, *Cont. Shelf*
415 *Res.*, 23, 387-391, 2003.

416 Cloern, J. E., Foster, S.Q. and Kleckner, A. E.: Phytoplankton primary production in the
417 world's estuarine-coastal ecosystems, *Biogeosciences*, 11, 2477-2501, 2014.

418 Doney, S. C., Busch, D. S., Cooley, S. R., and Kroeker, K. J.: The impacts of ocean
419 acidification on marine ecosystems and reliant human communities, *Annu. Rev. Env.*
420 *Resour.*, 45, 83-112, 2020.

421 [Du, C., He, R., Liu, Z., Huang, T., Wang, L., Yuan, Z., Xu, Y., Wang, Z. and Dai, M.:](#)
422 [Climatology of nutrient distributions in the South China Sea based on a large data](#)
423 [set derived from a new algorithm. *Prog. Oceanogr.*, 195, 102586, 2021.](#)

424 Dutkiewicz, S., Morris, J. J., Follows, M. J., Scott, J., Levitan, O., Dyhrman, S. T., and
425 Berman-Frank, I.: Impact of ocean acidification on the structure of future
426 phytoplankton communities, *Nat. Clim. Change*, 5, 1002-1006, 2015.

427 Eberlein, T., Wohrab, S., Rost, B., John, U., Bach, L. T., Riebesell, U., and Van de Waal,
428 D. B.: Effects of ocean acidification on primary production in a coastal North Sea
429 phytoplankton community, *Plos One*, 12, 1-15, 2017.

430 Endo, H., Sugie, K., Yoshimura, T., and Suzuki, K.: Effects of CO₂ and iron availability
431 on *rbcL* gene expression in Bering Sea diatoms, *Biogeosciences*, 12, 2247-2259,
432 2015.

433 Feng, Y., Hare, C. E., Rose, J. M., Handy, S. M., DiTullio, G. R., Lee, P. A., Smith, W. O.,

434 Peloquin, J., Tozzi, S., Sun, J., Zhang, Y., Dunbar, R. B., Long, M. C., Sohst, B.,
435 Lohan, M., and Hutchins, D. A.: Interactive effects of iron, irradiance and CO₂ on
436 Ross Sea phytoplankton, *Deep-Sea Res. PT. I*, 57, 368-383, 2010.

437 Flynn, K. J., Blackford, J. C., Baird, M. E., Raven, J. A., Clark, D. R., Beardall, J.,
438 Brownlee, C., Fabian, H., and Wheeler, G. L.: Changes in pH at the exterior surface
439 of plankton with ocean acidification, *Nat. Clim. Change*, 2, 510-513, 2012.

440 Gao, G., Xu, Z. G., Shi, Q., and Wu, H. Y.: Increased CO₂ exacerbates the stress of
441 ultraviolet radiation on photosystem II function in the diatom *Thalassiosira*
442 *weissflogii*, *Environ. Exp. Bot.*, 156, 96-105, 2018b.

443 ~~Gao, G., Gao, Q., Bao, M. L., Xu, J. T., and Li, X. S.: Nitrogen availability modulates the~~
444 ~~effects of ocean acidification on biomass yield and food quality of a marine crop~~
445 ~~*Pyropia yezoensis*, *Food Chem.*, 271, 623-629, 2019b.~~

446 Gao, G., Jin, P., Liu, N., Li, F. T., Tong, S. Y., Hutchins, D. A., and Gao, K. S.: The
447 acclimation process of phytoplankton biomass, carbon fixation and respiration to the
448 combined effects of elevated temperature and *p*CO₂ in the northern South China Sea,
449 *Mar. Pollut. Bull.*, 118, 213-220, 2017.

450 Gao, G., Qu, L., Xu, T., Burgess, J.G., Li, X. and Xu, J.: Future CO₂-induced ocean
451 acidification enhances resilience of a green tide alga to low-salinity stress. *ICES J.*
452 *Mar. Sci.*, 76, 2437-2445, 2019b.

453 Gao, G., Xia, J. R., Yu, J. L., Fan, J. L., and Zeng, X. P.: Regulation of inorganic carbon

带格式的: 下标

454 acquisition in a red tide alga (*Skeletonema costatum*): The importance of phosphorus
455 availability, *Biogeosciences*, 15, 4871-4882, 2018a.

456 Gao, K. S., Beardall, J., Häder, D. P., Hall-Spencer, J. M., Gao, G., and Hutchins, D. A.:
457 Effects of ocean acidification on marine photosynthetic organisms under the
458 concurrent influences of warming, UV radiation, and deoxygenation, *Front. Mar.*
459 *Sci.*, 6, 1-18, 2019a.

460 Gao, K. S., Xu, J. T., Gao, G., Li, Y. H., Hutchins, D. A., Huang, B. Q., Wang, L., Zheng,
461 Y., Jin, P., Cai, X. N., Hader, D. P., Li, W., Xu, K., Liu, N. N., and Riebesell, U.:
462 Rising CO₂ and increased light exposure synergistically reduce marine primary
463 productivity, *Nat. Clim. Change*, 2, 519-523, 2012.

464 Gattuso, J. P., Gao, K. S., Lee, K., Rost, B., and Schulz, K. G.: Approaches and tools to
465 manipulate the carbonate chemistry, pp 41-52. *Guide to best practices for ocean*
466 *acidification research and data reporting*, edited by: Riebesell, U., Fabry, V. J.,
467 Hansson, L., and Gattuso J.-P., Luxembourg: Publications Office of the European
468 Union, 2010.

469 Gattuso, J. P., Magnan, A., Billé R., Cheung, W. W. L., Howes, E. L., Joos, F., Allemand,
470 D., Bopp, L., Cooley, S. R., Eakin, C. M., Hoegh-Guldberg, O., Kelly, R. P., Portner,
471 H. O., Rogers, A. D., Baxter, J. M., Laffoley, D., Osborn, D., Rankovic, A., Rochette,
472 J., Sumaila, U. R., Treyer, S., and Turley, C.: Contrasting futures for ocean and
473 society from different anthropogenic CO₂ emissions scenarios, *Science*, 349,

474 aac4722, 2015.

475 Geider, R. J., La Roche, J., Greene, R. M., and Olaizola, M.: Response of the
476 photosynthetic apparatus of *Phaeodactylum tricornutum* (Bacillariophyceae) to
477 nitrate, phosphate, or iron starvation, *J. Phycol.*, 29, 755-766, 1993.

478 Häler, D. P., Williamson, C. E., Wängberg, S. A., Rautio, M., Rose, K. C., Gao, K. S.,
479 Helbling, E. W., Sinha, R. P., and Worrest, R.: Effects of UV radiation on aquatic
480 ecosystems and interactions with other environmental factors, *Photoch. Photobio.*
481 *Sci.*, 14, 108-126, 2015.

482 Hedges, J. I., and Keil, R. G.: Sedimentary organic matter preservation: an assessment
483 and speculative synthesis, *Mar. Chem.*, 49, 81-115, 1995.

484 Hein, M., and Sand-Jensen, K.: CO₂ increases oceanic primary production, *Nature*, 388,
485 526-527, 1997.

486 Hennon, G. M. M., Ashworth, J., Groussman, R. D., Berthiaume, C., Morales, R. L.,
487 Baliga, N. S., Orellana, M. V., and Armbrust, E. V.: Diatom acclimation to elevated
488 CO₂ via cAMP signalling and coordinated gene expression, *Nat. Clim. Change*, 5,
489 761-765, 2015.

490 Hofmann, G. E., Smith, J. E., Johnson, K. S., Send, U., Levin, L. A., Micheli, F., Paytan,
491 A., Price, N. N., Peterson, B., Takeshita, Y., Matson, P. G., Crook, E. D., Kroeker, K.
492 J., Gambi, M. C., Rivest, E. B., Frieder, C. A., Yu, P. C., and Martz, T. R.:
493 High-frequency dynamics of ocean pH: A multi-ecosystem comparison, *Plos One*, 6,

494 1-11, 2011.

495 Holding, J. M., Duarte, C. M., Sanz-Martín, M., Mesa, E., Arrieta, J. M., Chierici, M.,
496 Hendriks, I. E., Garcia-Corral, L. S., Regaudie-de-Gioux, A., Delgado, A., Reigstad,
497 M., Wassmann, P., and Agusti, S.: Temperature dependence of CO₂-enhanced
498 primary production in the European Arctic Ocean, *Nat. Clim. Change*, 5, 1079-1082,
499 2015.

500 Hong, H. S., Chai, F., Zhang, C. Y., Huang, B. Q., Jiang, Y. W., and Hu, J. Y.: An
501 overview of physical and biogeochemical processes and ecosystem dynamics in the
502 Taiwan Strait, *Cont. Shelf Res.*, 31, S3-S12, 2011.

503 Hong, H. Z., Shen, R., Zhang, F. T., Wen, Z. Z., Chang, S. W., Lin, W. F., Kranz, S. A.,
504 Luo, Y. W., Kao, S. J., Morel, F. M. M. and Shi, D. L.: The complex effects of ocean
505 acidification on the prominent N₂-fixing cyanobacterium *Trichodesmium*. *Science*,
506 356, 527-530, 2017.

507 Hopkinson, B. M., Dupont, C. L., Allen, A. E., and Morel, F. M.: Efficiency of the
508 CO₂-concentrating mechanism of diatoms, *P. Natl. Acad. Sci. USA.*, 108, 3830-3837,
509 2011.

510 Hoppe, C. J. M., Wolf, K. K. E., Schuback, N., Tortell, P. D., and Rost, B.: Compensation
511 of ocean acidification effects in Arctic phytoplankton assemblages. *Nat. Clim.*
512 *Change*, 8, 529-533, 2018.

513 [Hurd, C.L., Beardall, J., Comeau, S., Cornwall, C.E., Havenhand, J.N., Munday, P.L.,](#)

514 [Parker, L.M., Raven, J.A. and McGraw, C.M.: Ocean acidification as a multiple](#)
515 [driver: how interactions between changing seawater carbonate parameters affect](#)
516 [marine life. *Mar. Freshwater Res.*, 71, 263-274, 2019.](#)

517 [IPCC, 2019: IPCC Special Report on the Ocean and Cryosphere in a Changing Climate](#)
518 [\[H.-O. Pörtner, D.C. Roberts, V. Masson-Delmotte, P. Zhai, M. Tignor, E.](#)
519 [Poloczanska, K. Mintenbeck, A. Alegría, M. Nicolai, A. Okem, J. Petzold, B. Rama,](#)
520 [N.M. Weyer \(eds.\)\]. In press.](#)

521 Jin, P., Gao, G., Liu, X., Li, F. T., Tong, S. Y., Ding, J. C., Zhong, Z. H., Liu, N. N., and
522 Gao, K. S.: Contrasting photophysiological characteristics of phytoplankton
523 assemblages in the Northern South China Sea, *Plos One*, 11, 1-16, 2016.

524 Jin, P., Wang, T. F., Liu, N. N., Dupont, S., Beardall, J., Boyd, P. W., Riebesell, U., and
525 Gao, K. S.: Ocean acidification increases the accumulation of toxic phenolic
526 compounds across trophic levels, *Nat. Commun.*, 6, 1-6, 2015.

527 Johnson, M. D., and Carpenter, R. C.: Nitrogen enrichment offsets direct negative effects
528 of ocean acidification on a reef-building crustose coralline alga, *Biol. Letters*, 14,
529 1-5, 2018.

530 ~~[Lan, J., Hong, J. and Li, P.: Seasonal variability of cool core eddy in the Western South](#)~~
531 ~~[China Sea, *Adv. Earth Sci.*, 21, 1145-1152, 2006.](#)~~

532 Li, F. T., Wu, Y. P., Hutchins, D. A., Fu, F. X., and Gao, K. S.: Physiological responses of
533 coastal and oceanic diatoms to diurnal fluctuations in seawater carbonate chemistry

534 under two CO₂ concentrations, *Biogeosciences*, 13, 6247-6259, 2016.

535 Li, F. T., Beardall, J., and Gao, K. S.: Diatom performance in a future ocean: interactions
536 between nitrogen limitation, temperature, and CO₂-induced seawater acidification,
537 *ICES J. Mar. Sci.*, 75, 1451-1464, 2018.

538 Li, G., Gao, K. S., Yuan, D. X., Zheng, Y., and Yang, G. Y.: Relationship of
539 photosynthetic carbon fixation with environmental changes in the Jiulong River
540 estuary of the South China Sea, with special reference to the effects of solar UV
541 radiation, *Mar. Pollut. Bull.*, 62, 1852-1858, 2011.

542 Li, H. X., Xu, T. P., Ma, J., Li, F. T., and Xu, J. T.: Physiological responses of
543 *Skeletonema costatum* to the interactions of seawater acidification and the
544 combination of photoperiod and temperature, *Biogeosciences*, 18, 1439-1449, 2021.

545 Li, W., Gao, K., and Beardall, J.: Nitrate limitation and ocean acidification interact with
546 UV-B to reduce photosynthetic performance in the diatom *Phaeodactylum*
547 *tricornutum*, *Biogeosciences*, 12, 2383-2393, 2015.

548 [Lu, Z., Gan, J., Dai, M., Zhao, X. and Hui, C. R.: Nutrient transport and dynamics in the](#)
549 [South China Sea: A modeling study. *Prog. Oceanogr.*, 183, 102308, 2020.](#)

550 McNicholl, C., Koch, M. S., and Hofmann, L. C.: Photosynthesis and light-dependent
551 proton pumps increase boundary layer pH in tropical macroalgae: A proposed
552 mechanism to sustain calcification under ocean acidification, *J. Exp. Mar. Biol.*
553 *Ecol.*, 521, 1-12, 2019.

554 [Moreau, S., Penna, A. D., Llorc, J., Patel, R., Langlais, C., Boyd, P. W., Matear, R. J.,](#)
555 [Phillips, H. E., Trull, T. W., Tilbrook, B. and Lenton, A.: Eddy-induced carbon](#)
556 [transport across the Antarctic Circumpolar Current. *Global Biogeochem. Cy.*, 31,](#)
557 [1368-1386, 2017](#)

558 Mostofa, K.M., Liu, C.Q., Zhai, W., Minella, M., Vione, D., Gao, K., Minakata, D.,
559 Arakaki, T., Yoshioka, T., Hayakawa, K. and Konohira, E.: Reviews and Syntheses:
560 Ocean acidification and its potential impacts on marine ecosystems, *Biogeosciences*,
561 13, 1767-1786, 2016.

562 Pierrot, D., Wallace, D.W. R., and Lewis, E.: MS Excel program developed for CO₂
563 system calculations. ORNL/CDIAC-105a, Carbon Dioxide Information Analysis
564 Center, Oak Ridge National Laboratory, US Department of Energy, Oak Ridge,
565 Tennessee, USA., 2006.

566 Porra, R. J.: The chequered history of the development and use of simultaneous equations
567 for the accurate determination of chlorophylls a and b, *Photosynth. Res.*, 73,
568 149-156, 2002.

569 Raven, J. A., and Beardall, J.: CO₂ concentrating mechanisms and environmental change,
570 *Aquat. Bot.*, 118, 24-37, 2014.

571 Schippers, P., Lüring, M., and Scheffer, M.: Increase of atmospheric CO₂ promotes
572 phytoplankton productivity, *Ecol. Lett.*, 7, 446-451, 2004.

573 Shi, D. L., Hong, H. Z., Su, X., Liao, L. R., Chang, S. W., and Lin, W. F.: The

574 physiological response of marine diatoms to ocean acidification: Differential roles of
575 seawater $p\text{CO}_2$ and pH, *J. Phycol.*, 55, 521-533, 2019.

576 ~~Sugie, K., Fujiwara, A., Nishino, S., Kameyama, S. and Harada, N.: Impacts of~~
577 ~~temperature, CO_2 , and salinity on phytoplankton community composition in the~~
578 ~~Western Arctic Ocean, *Front. Mar. Sci.*, 6, 1-17, 2020.~~

579 Taylor, A. R., Brownlee, C., and Wheeler, G. L.: Proton channels in algae: Reasons to be
580 excited, *Trends Plant Sci.*, 17, 675-684, 2012.

581 Tortell, P. D., Rau, G. H., and Morel, F. M. M.: Inorganic carbon acquisition in coastal
582 Pacific phytoplankton communities, *Limnol. Oceanogr.*, 45, 1485-1500, 2000.

583 Tremblay, J. E., Michel, C., Hobson, K. A., Gosselin, M., and Price, N. M.: Bloom
584 dynamics in early opening waters of the Arctic Ocean. *Limnol. Oceanogr.*, 51,
585 900-912, 2006.

586 Riebesell, U., Aberle-Malzahn, N., Achterberg, E. P., Algueró-Muñiz, M.,
587 Alvarez-Fernandez, S., Arístegui, J., Bach, L. T., Boersma, M., Boxhammer, T.,
588 Guan, W. C., Haunost, M., Horn, H. G., Loscher, C. R., Ludwig, A., Spisla, C.,
589 Sswat, M., Stange, P., and Taucher, J.: Toxic algal bloom induced by ocean
590 acidification disrupts the pelagic food web, *Nat. Clim. Change*, 8, 1082-1086, 2018.

591 Wu, Y., Gao, K., and Riebesell, U.: CO_2 -induced seawater acidification affects
592 physiological performance of the marine diatom *Phaeodactylum tricorutum*,
593 *Biogeosciences*, 7, 2915-2923, 2010.

594 Wu, Y., Campbell, D. A., Irwin, A. J., Suggett, D. J., and Finkel, Z. V.: Ocean
595 acidification enhances the growth rate of larger diatoms. *Limnol. Oceanogr.*, 59,
596 1027-1034, 2014.

597 Wu, Y. P., and Gao, K. S.: Combined effects of solar UV radiation and CO₂-induced
598 seawater acidification on photosynthetic carbon fixation of phytoplankton
599 assemblages in the South China Sea. *Chinese Sci. Bull.*, 55, 3680-3686, 2010.

600 ~~Wulff, A., Karlberg, M., Olofsson, M., Torstensson, A., Riemann, L., Steinhoff, F. S.,
601 Mohlin, M., Ekstrand, N., and Chierici, M.: Ocean acidification and desalination:
602 Climate-driven change in a Baltic Sea summer microplanktonic community, *Mar.
603 Biol.*, 165, 1-15, 2018.~~

604 Xiao, W. P., Wang, L., Laws, E., Xie, Y. Y., Chen, J. X., Liu, X., Chen, B. Z., and Huang,
605 B. Q.: Realized niches explain spatial gradients in seasonal abundance of
606 phytoplankton groups in the South China Sea, *Prog. Oceanogr.*, 162, 223-239, 2018.

607 Xie, S., Lin, F., Zhao, X. and Gao, G.: Enhanced lipid productivity coupled with carbon
608 and nitrogen removal of the diatom *Skeletonema costatum* cultured in the high CO₂
609 level. *Algal Res.* 61, 102589, 2022.

610 Xu, J. K., Sun, J. Z., Beardall, J., and Gao, K. S.: Lower salinity leads to improved
611 physiological performance in the coccolithophorid *Emiliana huxleyi*, which partly
612 ameliorates the effects of ocean acidification, *Front. Mar. Sci.*, 7, 1-18, 2020.

613 Xu, Z. G., Gao, G., Xu, J. T., and Wu, H. Y.: Physiological response of a golden tide alga

带格式的: 字体: 倾斜

带格式的: 下标

614 (*Sargassum muticum*) to the interaction of ocean acidification and phosphorus
615 enrichment, *Biogeosciences*, 14, 671-681, 2017.

616 Yang, G. Y., and Gao, K. S.: Physiological responses of the marine diatom *Thalassiosira*
617 *pseudonana* to increased $p\text{CO}_2$ and seawater acidity, *Mar. Environ. Res.*, 79,
618 142-151, 2012.

619 Yoshimura, T., Nishioka, J., Suzuki, K., Hattori, H., Kiyosawa, H. and Watanabe, Y. W.:
620 Impacts of elevated CO_2 on organic carbon dynamics in nutrient depleted Okhotsk
621 Sea surface waters. *J. Exp. Mar. Biol. Ecol.*, 395, 191-198, 2010.

622 Yu, P., Wang, Z. A., Churchill, J., Zheng, M., Pan, J., Bai, Y. and Liang, C.: Effects of
623 typhoons on surface seawater $p\text{CO}_2$ and air-sea CO_2 fluxes in the northern South
624 China Sea. *J. Geophys. Res-Oceans*, 125, p.e2020JC016258, 2020.

625 Yuan, X., He, L., Yin, K., Pan, G. and Harrison, P. J.: Bacterial distribution and nutrient
626 limitation in relation to different water masses in the coastal and northwestern South
627 China Sea in late summer. *Cont. Shelf Res.*, 31, 1214-1223, 2011.

628 Zhong, Y. P., Liu, X., Xiao, W. P., Laws, E. A., Chen, J. X., Wang, L., Liu, S. G., Zhang,
629 F., and Huang, B. Q.: Phytoplankton community patterns in the Taiwan Strait match
630 the characteristics of their realized niches, *Prog. Oceanogr.*, 186, 1-15, 2020.

带格式的: 下标
带格式的: 下标

631 **Figure captions**

632 **Fig. 1** Sampling stations for the incubation experiments in the Taiwan Strait and the
633 South China Sea during three cruises. Taiwan Strait cruise was conducted in July 2016
634 (red dots), South China Sea Basin cruise were conducted in September 2016 (blue dots)
635 and Western South China Sea cruise was conducted in September 2017 (black dots). ~~The~~
636 ~~arrows represent surface circulation fields in summer in the vicinity of Vietnam coast~~
637 ~~based on Lan et al. (2006).~~

638 **Fig. 2** Temperature ($^{\circ}\text{C}$, panel a), salinity (panel b), pH (panel c), total alkalinity (μmol
639 L^{-1} , panel d), and CO_2 ($\mu\text{mol kg}^{-1}$ SW, panel e) in surface seawater and mean PAR
640 intensity ($\text{W m}^{-2} \text{s}^{-1}$, panel f) during the PP incubation experiments.

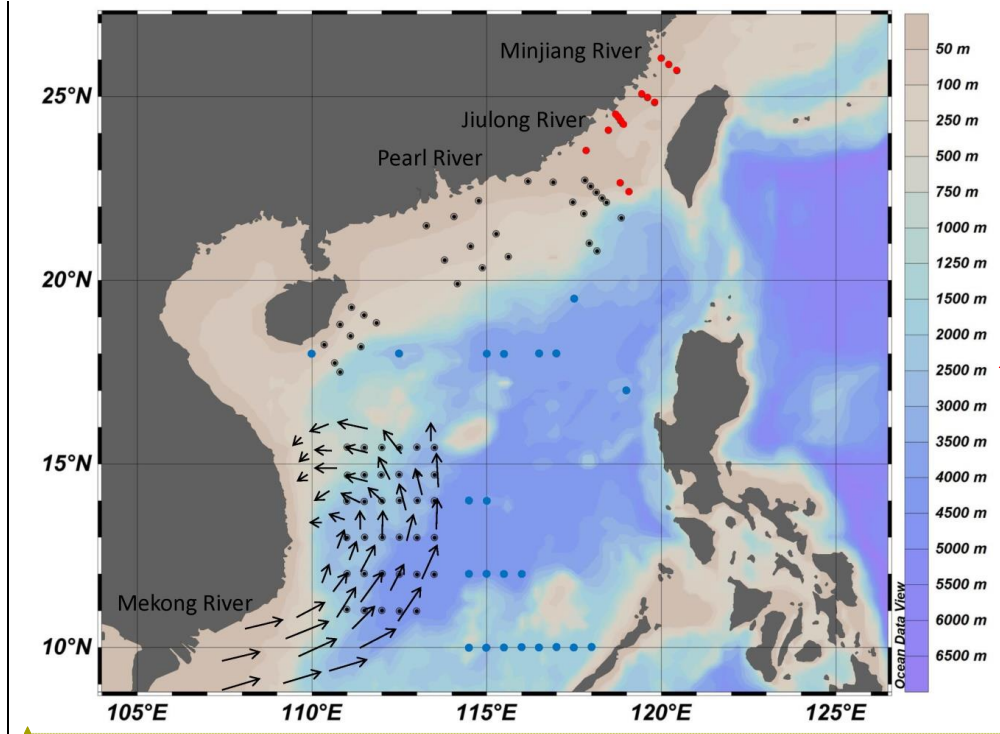
641 **Fig. 3** Chl *a* concentration ($\mu\text{g L}^{-1}$) in the Taiwan Strait and the South China Sea during
642 research cruises.

643 **Fig. 4** Surface primary productivity ($\mu\text{g C } (\mu\text{g Chl } a)^{-1} \text{ d}^{-1}$) in the Taiwan Strait and the
644 South China Sea during research cruises.

645 **Fig. 5** Ocean acidification (pH decreases of 0.4 units) induced changes (%) of surface
646 primary productivity in the Taiwan Strait and the South China Sea. Red-yellow shading
647 represents a positive effect on PP and blue-purple shading represents a negative effect.

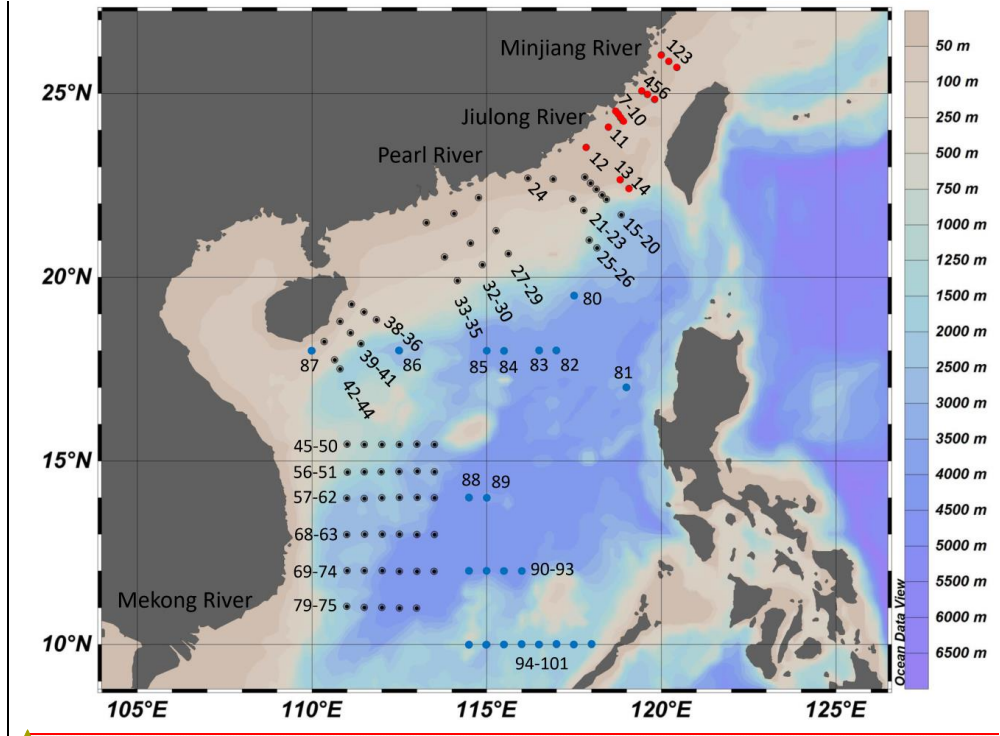
648 ~~Positive effect was found in coastal waters and estuary affected waters, such as the~~
649 ~~Taiwan Strait, the Pearl River plume, Mekong River induced Rip current in West China~~
650 ~~Sea. Negative effect was found in surface of oligotrophic waters like SCS Basin.~~

Fig. 6 Ocean acidification (pH decreases of 0.4 units) induced changes (%) on surface primary productivity in the South China Sea as a function of ~~salinity (a), PAR (b),~~ ambient pH (ea), ~~PAR (b),~~ and ~~salinity (c)nitrate plus nitrite concentration (d)~~. The dotted lines represent 95% confidence intervals.



带格式的: 字体: (默认) Times
New Roman, 小四

带格式的: 缩进: 左侧: 0 厘米,
悬挂缩进: 2 字符



带格式的: 字体: (默认) Times
New Roman, 小四

Fig. 1

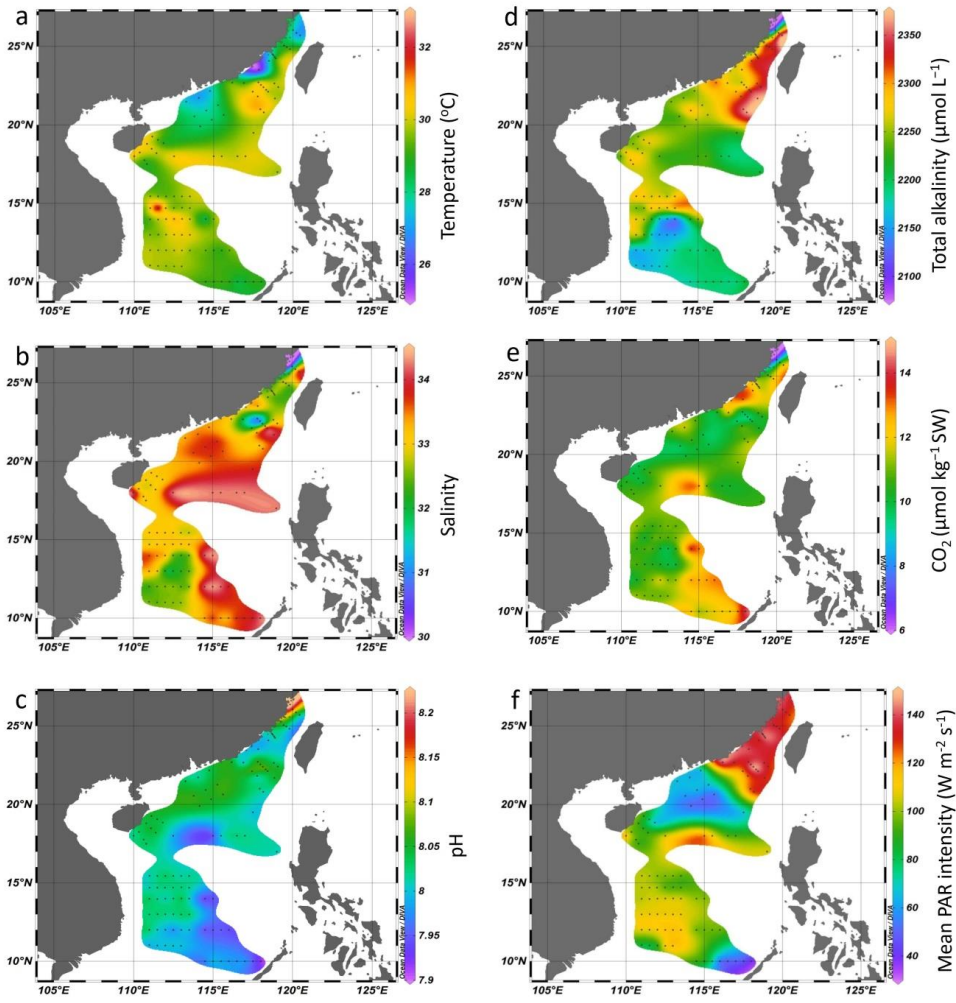


Fig. 2

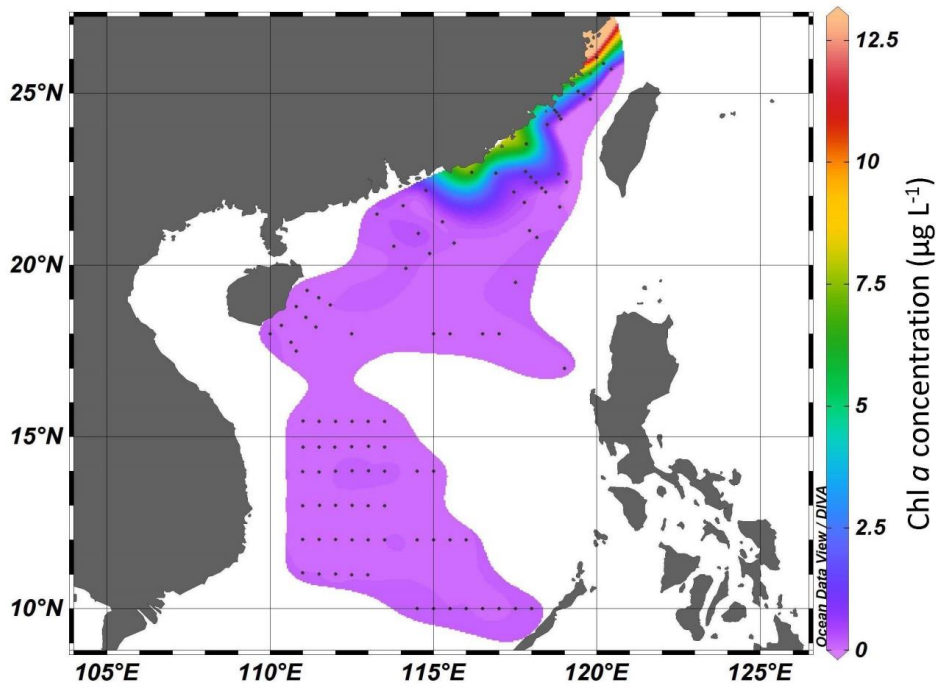


Fig. 3

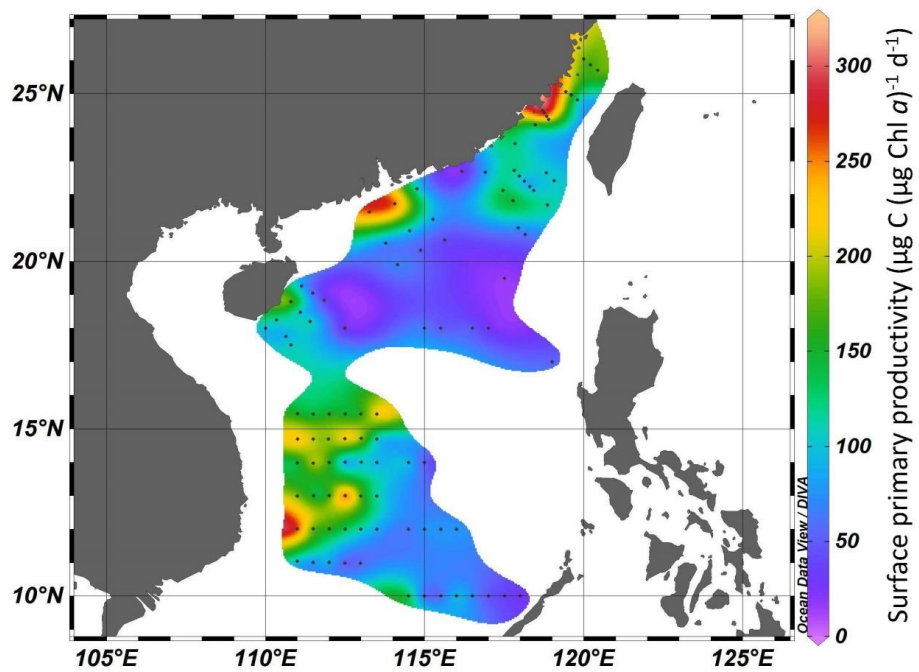


Fig. 4

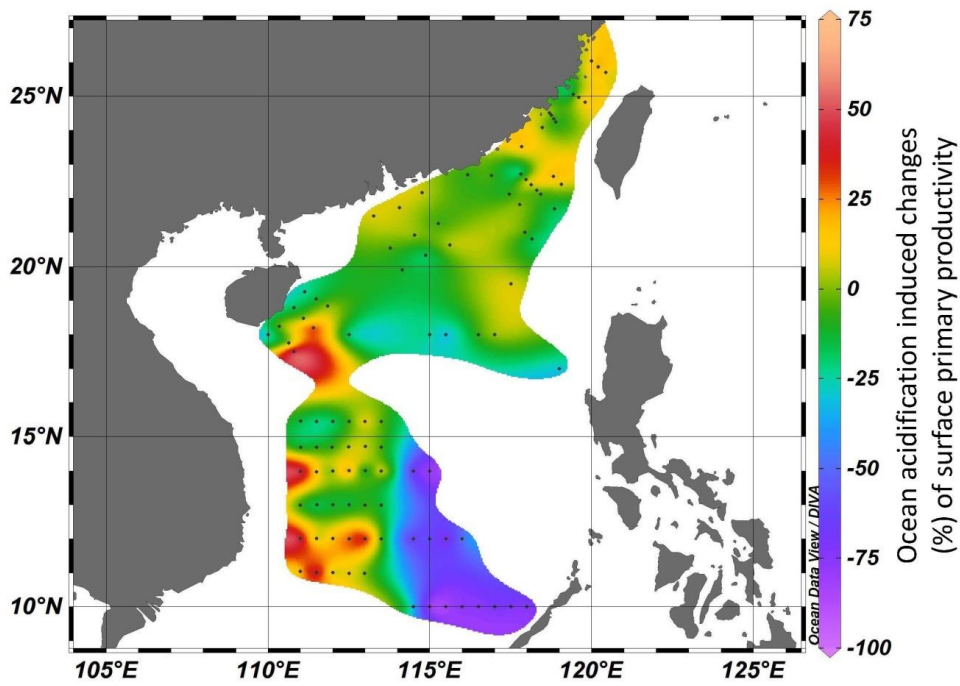
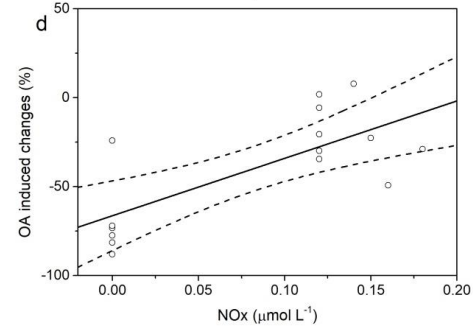
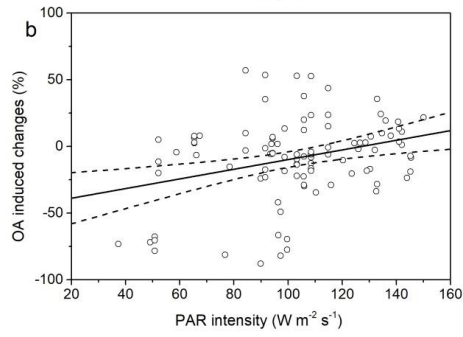
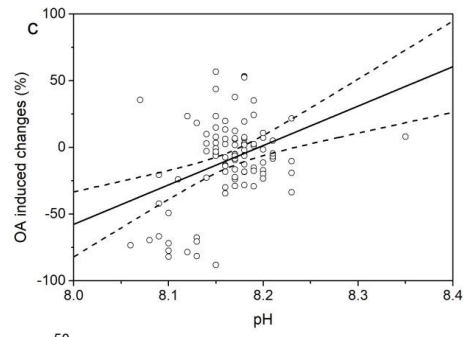
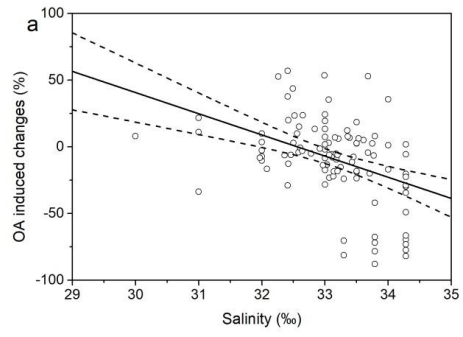
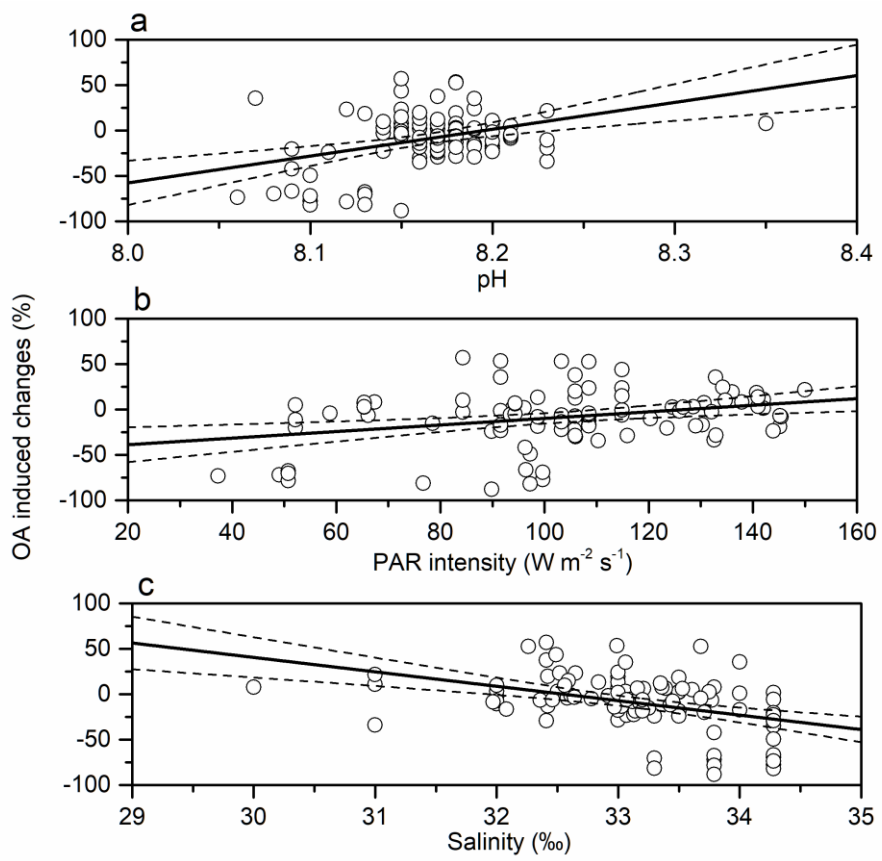


Fig. 5





带格式的: 字体: (默认) Times
New Roman, 小四

带格式的: 缩进: 左侧: 0 厘米,
悬挂缩进: 2 字符

Fig. 6